

Predicted levels of ${}^9\text{Be}$ based on a theoretical analysis of neutron double-differential cross sections at $E_n = 14.1$ and 18 MeV

Junfeng Duan, Jingshang Zhang, and Haicheng Wu

China Institute of Atomic Energy, P. O. Box 275(41), Beijing 102413, People's Republic of China

Xiaojun Sun*

College of Physics and technology, Guangxi Normal University, Guilin 541004, People's Republic of China

(Received 30 October 2009; published 30 December 2009)

By using the statistical theory for neutron-induced light nucleus reaction, the calculation of the neutron double-differential cross sections for $n + {}^9\text{Be}$ reactions is performed. The secondary outgoing neutrons only coming from the $(n, 2n)2\alpha$ reaction channel through six different emission processes are illustrated in detail in this article. Based on the theoretical analysis of neutron double-differential cross sections at $E_n = 14.1$ and 18 MeV, two predicted levels of ${}^9\text{Be}$, i.e., $E(J^\pi)\Gamma = 9(\frac{3}{2}^+)1000$ and $10(\frac{3}{2}^+)1000$, have been recommended. The calculated results indicate that the fittings would be improved obviously while the predicted levels have been employed.

DOI: [10.1103/PhysRevC.80.064612](https://doi.org/10.1103/PhysRevC.80.064612)

PACS number(s): 24.10.-i, 25.40.-h, 28.20.Cz

I. INTRODUCTION

Because of the relatively large $(n, 2n)$ cross section, low mass, and low neutron-capture cross section, ${}^9\text{Be}$ has long been selected as the material for improving neutron economy in thermal and fast-fission reactors and in the design of accelerator-driven spallation neutron sources, as the plasma facing material of the first wall in ITER, and as a neutron multiplier in the fusion blanket. Therefore, the data for $n + {}^9\text{Be}$ reaction, especially neutron double-differential cross sections, are essential.

There are a number of measurements of the outgoing neutron double-differential cross section of ${}^9\text{Be}$ in earlier years, such as by Drake *et al.* [1] in 1977, Baba *et al.* [2] in 1983, Takahashi *et al.* [3] in 1983 (their results were published in 1988 [4]), Baba *et al.* [5] in 1988, and Qi Bu-Jia *et al.* [6] in 1995. In 1998, Ibaraki and Baba *et al.* [7] measured the same data of ${}^9\text{Be}$ again for several incident energies in the range 11.5–18 MeV. In 2007, Ruan Xi-Chao *et al.* [8] published the measured outgoing neutron double-differential cross section of ${}^9\text{Be}$, and Schmidt *et al.* [9] measured the same data at energies between 7.10 and 9.97 MeV. Recently, Jinxiang Chen *et al.* [10] published the same data at 5.9 and 6.4 MeV incident neutron. These data will provide abundant proofs to verify the reasonable reaction model and to probe the more accurate nuclear structure.

However, the evaluation or model calculation of outgoing neutron double-differential cross section are not satisfactory. Because there is lack of the appropriate theoretical method, the Monte Carlo technique was used by Perkins *et al.* [11] in 1985. It is worth mentioning that their calculated spectra were adopted in ENDF/B-VI, even in ENDF/B-VII. This evaluation method assumed that the reaction proceeded as a series of time-sequential reactions through levels in ${}^9\text{Be}$, ${}^8\text{Be}$, ${}^6\text{He}$, and ${}^5\text{He}$. The inconsistency of this method is at high incident energies

and backward angles. The theoretical model of the ${}^9\text{Be}(n, 2n)$ double-differential cross section is proposed by Beynon *et al.* [12] assuming isotopic center-of-mass distributions at each of the reaction stages and zero contribution from three-body breakup. The calculated results were obviously overestimated, especially in the low-incident-energy region. In 1995, SUN Wei-Li *et al.* [13] gave the formulas of the double-differential cross section of $n + {}^9\text{Be}$ reaction using dynamics and the quasi-free scattering approach assuming the isotopic neutron angular distribution. In 1997, Pronyaev *et al.* [14] proposed the least-squares product for determination of the contribution of each reaction mechanism in terms of fitting the measured data, but this method does not consider the theoretical background and their results are not adopted by any Evaluated Nuclear Data Library.

Although much effort has been made during the past several decades, there is lack of a general theory or method that can satisfactorily reproduce the measured neutron double-differential cross sections, including all incident energies mentioned above. This problem originates from two main sources. First, the description of the emission process from a compound nucleus to the discrete levels of the residual nuclei with pre-equilibrium mechanism, which dominates the light nucleus reactions, is absent in theoretical method. Second, level schemes of target nuclide ${}^9\text{Be}$, and the residual nuclide such as ${}^8\text{Be}$, ${}^6\text{He}$, and ${}^5\text{He}$ in many channels especially in ${}^9\text{Be}(n, 2n)$ channel, are absent or not accurate. Fortunately, the settlement of these two problems is feasible. The new level schemes of $A = 5-7$ [15] and $A = 8-10$ [16] were published by Tilley *et al.* in 2002 and in 2004, respectively, and the statistical theory for neutron-induced light nucleus reaction was proposed in 1999 [17] and improved in 2009 by Jingshang ZHANG [18].

Levels of the target and residual nucleus for $n + {}^9\text{Be}$ reaction have great effects on the particle emission, especially on the neutron double-differential cross sections. Table I lists the energy level schemes of the target nuclide ${}^9\text{Be}$ published in 2004 [16] and 1996 [19], respectively. As shown

* sxj0212@mailbox.gxnu.edu.cn

TABLE I. The comparison of the level schemes for ^9Be . The data are taken from the *Table of Isotopes, 8th ed.*, published in 1996 [19] and from Ref. [16], published in 2004. The format is $E(J^\pi)\Gamma$, where E is energy in MeV, J^π the spin and the parity, and Γ the energy width in keV.

2004 [16]	1996 [19]
g.s. ($\frac{3}{2}^-$) stable	g.s. ($\frac{3}{2}^-$) stable
1.684 ($\frac{1}{2}^+$) 217	1.684 ($\frac{1}{2}^+$) 217
2.4294 ($\frac{5}{2}^-$) 0.78	2.4294 ($\frac{5}{2}^-$) 0.77
2.78 ($\frac{1}{2}^-$) 1080	2.78 ($\frac{1}{2}^-$) 1080
3.049 ($\frac{3}{2}^+$) 282	3.049 ($\frac{3}{2}^+$) 282
4.704 ($\frac{3}{2}^+$) 743	4.704 ($\frac{3}{2}^+$) 743
5.59 ($\frac{3}{2}^-$) 1330	
6.38 ($\frac{7}{2}^-$) 1210	
6.76 ($\frac{9}{2}^+$) 1330	6.76 ($\frac{7}{2}^-$) 1540
7.94 ($\frac{5}{2}^-$) 1000	7.94 ($\frac{5}{2}^-$) 1000
9.00 ($\frac{5}{2}^+$) 1000*	
10.00 ($\frac{5}{2}^+$) 1000*	
11.283 ($\frac{7}{2}^-$) 575	11.283 (?) 575
11.81 ($\frac{5}{2}^-$) 400	11.81 (?) 400
13.79 (?) 590	13.79 (?) 590
14.3922 ($\frac{3}{2}^-$) 0.381	14.3922 ($\frac{3}{2}^-$) 0.381
14.48 ($\frac{3}{2}^-$) 800	14.40 (?) 800
15.10 (?) 350	15.10 (?) ?
15.97 (?) 300	15.97 (?) 300
16.671 ($\frac{5}{2}^-$) 41	16.671 ($\frac{5}{2}^-$) 41
16.9752 ($\frac{1}{2}^-$) 0.389	16.9752 ($\frac{1}{2}^-$) 0.49
17.298 ($\frac{5}{2}^-$) 200	17.298 ($\frac{5}{2}^-$) 200
17.493 ($\frac{7}{2}^+$) 47	17.493 ($\frac{7}{2}^+$) 47

*Labels the predicted energy levels in this article. g.s. + ground state; indicates the absent data.

in Table I, two new levels, i.e., $E(J^\pi)\Gamma = 5.59(\frac{3}{2}^-)1330$ and $6.38(\frac{7}{2}^-)1210$ are added, and the spins, parities, and energy widths of some previous energy levels are recognized. Furthermore, for the residual nuclide ^5He as listed in Table II, the previous level $E(J^\pi)\Gamma = 4.0(\frac{1}{2}^-)400$ is replaced by a new level $E(J^\pi)\Gamma = 1.27(\frac{1}{2}^-)5570$. At the same time, four new levels $E(J^\pi)\Gamma = 16.84(\frac{3}{2}^+)745$, $19.14(\frac{5}{2}^+)3500$, $19.26(\frac{3}{2}^+)3960$, and $19.31(\frac{7}{2}^+)3020$ are added and the previous levels $E(J^\pi)\Gamma = 16.75(\frac{3}{2}^+)76$ and $19.8(\frac{3}{2}, \frac{5}{2}^+)2550$ are erased. For the residual nuclide ^6He as also shown in Table II, the new level $E(J^\pi)\Gamma = 5.6(2^+)12100$ is added, and the previous level $E(J^\pi)\Gamma = 13.6(1^-, 2^-)?$ is replaced by the new level $E(J^\pi)\Gamma = 14.6(1^-)7400$. This alteration implies that all of the energy position of the outgoing particle spectra related with those levels has been shifted accordingly. For the intermediary nucleus ^8Be , the variation of its level schemes published in 1996 [19] and 2004 [16] is too little. These updated energy level schemes mentioned above, significantly improve the calculated neutron double-differential cross sections below the 10-MeV incident energy in our latest studies [10,20]

TABLE II. The comparison of the level schemes for ^5He and ^6He . The data are taken from the *Table of Isotopes, 8th ed.*, published in 1996 [19] and from Ref. [15], published in 2002. The format is consistent with the Table I.

2002 [15]	1996 [19]
^5He	
g.s. ($\frac{3}{2}^-$) 648	g.s. ($\frac{3}{2}^-$) 600
1.27 ($\frac{1}{2}^-$) 5570	
16.84 ($\frac{3}{2}^+$) 75	4.0 ($\frac{1}{2}^-$) 4000
19.14 ($\frac{5}{2}^+$) 3560	16.75 ($\frac{3}{2}^+$) 76
19.26 ($\frac{3}{2}^+$) 3960	
19.31 ($\frac{7}{2}^+$) 3020	
	19.8 ($\frac{3}{2}, \frac{5}{2}^+$) 2550
^6He	
g.s. (0^+) 806.7 ms	g.s. (0^+) 806.7 ms
1.797 (2^+) 113	1.797 (2^+) 113
5.6 (2^+) 12100	
	13.6 ($1^-, 2^-$) ?
14.6 (1^-) 7400	
15.5 (?) 4000	15.5 (?) 4000

g.s. = ground state; ? indicates the absent data.

using the statistical theory for neutron-induced light nucleus reaction [18].

However, the calculated neutron double-differential cross sections at 10–20 MeV incident energy do not correlate well with the measured data, because there may be still absent energy levels of the target nucleus. One can see in Table I that the energy interval between the 9th excited state and the 10th excited state is up to 3.343 MeV. This value is not only much higher than the average energy interval but also is not explained by the energy band theory. Therefore, we predict that there may be two new energy levels between $E(J^\pi)\Gamma = 7.94(\frac{5}{2}^-)1000$ and $11.238(\frac{7}{2}^+)575$. On the basis of the statistical theory [18], we calculate the neutron double differential cross sections at 14.1 and 18 MeV incident energies using the updated energy levels, while two predicted energy levels are (or not) employed. The results show that two predicted energy levels, i.e., $E(J^\pi)\Gamma = 9(\frac{5}{2}^+)1000$ and $10(\frac{5}{2}^+)1000$ as labeled asterisk in Table I, obviously improve the agreement with the experimental data.

This article proceeds as follow. In Sec. II, the statistical theory for neutron-induced light nucleus reaction is briefly introduced. The channels of $n + ^9\text{Be}$ reaction are analyzed in detail in the next section. In Sec. IV, the comparisons are performed between the model calculation and the experimental data, while two predicted energy levels are (or not) employed. In the last section a summary is given.

II. THEORETICAL MODEL

In light nucleus reaction model, the probability of all kinds of emitted particles could be given by dynamics and the shape

of spectra for various emitted particles could be produced by kinematics. The phenomenological spherical optical potential is employed in the model calculations. And the optical model parameters of neutrons and charged particles are determined by various cross section.

A. Dynamics

Early researches [21–29] indicate that the pre-equilibrium emission process from a compound nucleus to discrete levels of residual nuclei is the dominative reaction mechanism in neutron-induced light nucleus reaction. The light nucleus reaction model [17] could describe this dominative reaction mechanism very well. In this model the formula of energy spectrum reads as follows

$$\frac{d\sigma}{d\varepsilon} = \sum_{J\pi} \sigma_a^{J\pi} \sum_n P^{J\pi}(n) \frac{W_b^{J\pi}(n, E, \varepsilon)}{W_T^{J\pi}(n, E)}, \quad (1)$$

where $\sigma_a^{J\pi}$ refers to the absorption cross section, $P^{J\pi}(n)$ stands for the occupation probability of the n exciton state in the $J\pi$ channel, $W_b^{J\pi}(n, E, \varepsilon)$ is the emission rate of particle b at n exciton state with outgoing energy ε , and $W_T^{J\pi}(n, E)$ is the total emission rate with incident neutron energy E . The more light the nucleus is, the more important its pre-equilibrium emission item $W_b^{J\pi}(n, E, \varepsilon)$ is, which is written as [30–32]

$$W_b^{J\pi}(n, E, \varepsilon) = \frac{1}{2\pi\hbar} \sum_{jl} \sum_{l'\pi'} T_{jl}^b(\varepsilon) \Delta(JjI') f_l(\pi\pi') \times \sum_{\lambda} F_{b[\lambda, m]}(\varepsilon) Q_{b[\lambda, m]}(\varepsilon) \frac{\delta(E' - E'_b)}{\omega^{J\pi}(n, E)}. \quad (2)$$

Here E' , I' , and π' denote respectively energy, spin and parity of the final discrete level state, and E'_b stands for the residual excitation energy. T_{jl}^b is transmission coefficients of l partial wave that can be calculated by optical model. $\Delta(JjI')$ refers to the angular-momentum triangle relationship and $f_l(\pi\pi')$ is parity factor to keep the parity conservation. The factor $F_{b[\lambda, m]}$ stands for the preformation probability of configuration $[\lambda, m]$ for emitted particle b in compound nucleus, which means that the outgoing composite particle is constitutive of λ nucleons above the Fermi surface and the m nucleons below the Fermi surface. Of course, the preformation probability is 1 for neutron and proton. The preformation probability of ${}^5\text{He}$ cluster and its emission have been taken into account in this model [33]. It is well known that the unstable ${}^5\text{He}$ cluster can be separated into neutron and α spontaneously. $Q_{b[\lambda, m]}$ stands for the combination factor to distinguish between neutron and proton in $[\lambda, m]$ configuration. $\omega^{J\pi}(n, E)$ is the state density of n exciton state with the excited energy E^* of compound nucleus, which depends linearly on the incident energy E .

B. Kinematics

There is very strong recoil effect in light nucleus reaction because of the light mass. Therefore the kinematics of various particles emission must be taken into account strictly. The

accurate kinematics can not only produce the reasonable shape of the spectra but also keep the energy balance. The formula proposed by Ohlsen [34] is used to describe the direct three-body breakup process. The secondary particle double-differential cross sections from the discrete levels and the two-body breakup process of the unstable residual cluster have been analytically given in Ref. [17]. The formula of the three-body breakup process from a residual nucleus has also been given [21,22]. Because ${}^5\text{He}$ is a fermion, the orbit angular momentum of the ${}^{10}\text{Be} \rightarrow {}^5\text{He} + {}^5\text{He}$ process must be even. The double-differential cross sections of the neutron and α particle from ${}^5\text{He} \rightarrow n + \alpha$ breakup process are given in the Appendix.

III. REACTION CHANNELS

In view of $n + {}^9\text{Be}$ reactions with incident neutron energy $E_n \leq 20$ MeV, the opened reaction channels and the corresponding reaction Q values and the threshold energy E_{th} in unit of MeV are listed as Eq. (3).

$$n + {}^9\text{Be} \rightarrow \begin{cases} \gamma + {}^{10}\text{Be} & Q = 6.811 & E_{\text{th}} = 0.000 \\ p + {}^9\text{Li} & Q = -12.825 & E_{\text{th}} = 14.260 \\ \alpha + {}^6\text{He} & Q = -0.598 & E_{\text{th}} = 0.665 \\ d + {}^8\text{Li} & Q = -14.663 & E_{\text{th}} = 16.304 \\ t + {}^7\text{Li} & Q = -10.439 & E_{\text{th}} = 11.604 \\ {}^5\text{He} + {}^5\text{He} & Q = -3.362 & E_{\text{th}} = 3.738 \\ 2n + {}^8\text{Be} & Q = -1.665 & E_{\text{th}} = 1.851 \\ np, pn + {}^8\text{Li} & Q = -16.887 & E_{\text{th}} = 18.777 \\ n\alpha, \alpha n + {}^5\text{He} & Q = -2.467 & E_{\text{th}} = 2.743 \\ nd, dn + {}^7\text{Li} & Q = -16.696 & E_{\text{th}} = 18.565 \\ nt, tn + {}^6\text{Li} & Q = -17.688 & E_{\text{th}} = 19.668. \end{cases} \quad (3)$$

The first excited level of ${}^9\text{Be}$ is 1.684 MeV, but the binding energy of neutron in ${}^9\text{Be}$ is only 1.665 MeV. Therefore, the first excited level of ${}^9\text{Be}$ can emit neutrons with the residual nucleus ${}^8\text{Be}$, which is unstable and can be separated into two α particles spontaneously. Thus, this reaction is one of the decay modes to the ${}^9\text{Be}(n, 2n)2\alpha$ reaction channel. The capture cross section of ${}^9\text{Be}$ is very small. The compound nucleus ${}^{10}\text{Be}$ can be separated into two neutrons and ${}^8\text{Be}$ through direct three body breakup process, which also belongs to the ${}^9\text{Be}(n, 2n)2\alpha$ reaction channel since ${}^8\text{Be}$ can be separated into two α particles spontaneously. The residual nucleus ${}^6\text{He}$ is yielded through the first α emission. Of course the α emission leaving ${}^6\text{He}$ in the ground belongs to (n, α) reaction channel. While the α emission leaving ${}^6\text{He}$ in the first excited state, of which the excited energy (only 1.797 MeV) is lower than its neutron binding energy (1.860 MeV), therefore ${}^6\text{He}$ only decays through three body break-up process ${}^6\text{He} \rightarrow n + n + \alpha$ and contributes to ${}^9\text{Be}(n, 2n)2\alpha$ channel. Furthermore, the second excited level of ${}^6\text{He}$ can emit neutron with the residual nucleus ${}^5\text{He}$, which can be separated into the neutron and α particle spontaneously mentioned above, so this process still belongs to the ${}^9\text{Be}(n, 2n)2\alpha$ channel. Meanwhile the double two-body breakup process of the $(n, {}^5\text{He}){}^5\text{He}$ and $(n, n\alpha){}^5\text{He}$ reactions also belong to the ${}^9\text{Be}(n, 2n)2\alpha$ reaction channel. The reaction mechanisms to ${}^9\text{Be}(n, 2n)2\alpha$ channel

involved in the model calculation are shown in Eq. (4), where the symbol k refers to the order number of the excited

level of the corresponding residual nucleus in the different reaction channels.

$$n + {}^9\text{Be} \rightarrow {}^{10}\text{Be}^* \rightarrow \begin{cases} n + {}^9\text{Be}^* & {}^9\text{Be}_{k=1-3}^* \rightarrow n + {}^8\text{Be}^* & {}^8\text{Be}^* \rightarrow \alpha + \alpha \text{ two body breakup} \\ n + {}^9\text{Be}^* & {}^9\text{Be}_{k \geq 4}^* \rightarrow \alpha + {}^5\text{He}^* & {}^5\text{He}^* \rightarrow n + \alpha \text{ two body breakup} \\ \alpha + {}^6\text{He}^* & {}^6\text{He}_{k=1}^* \rightarrow n + n + \alpha & \text{three body breakup} \\ \alpha + {}^6\text{He}^* & {}^6\text{He}_{k \geq 2}^* \rightarrow n + {}^5\text{He}^* & {}^5\text{He}^* \rightarrow n + \alpha \text{ two body breakup} \\ {}^5\text{He}^* + {}^5\text{He}^* & {}^2{}^5\text{He}^* \rightarrow 2n + 2\alpha & \text{double two body breakup} \\ n + n + {}^8\text{Be}^* & \text{direct three body breakup} & {}^8\text{Be}^* \rightarrow \alpha + \alpha \text{ two body breakup.} \end{cases} \quad (4)$$

IV. CALCULATED RESULTS AND ANALYSIS

The LUNF code [17] based on the light nucleus reaction model for $n + {}^9\text{Be}$ reactions has been developed and used for calculating all kinds of the reaction cross sections, the angular distributions, and the double-differential cross sections of all kinds of outgoing particles from each partial reaction channel.

In $n + {}^9\text{Be}$ reaction, the total outgoing neutron energy-angular spectrum mainly comes from the contribution of the $(n, 2n)2\alpha$ reaction, as given by Eq. (4), which include six reaction mechanisms. As an example, for $\theta_L = 80^\circ$ at $E_n = 18$ MeV, the partial spectra of the emitted neutron from $(n, 2n) {}^8\text{Be}^*$ and direct three body breakup of ${}^6\text{He}$ and ${}^{10}\text{Be}$ are shown in Fig. 1. And the ones from $(n, n\alpha) {}^5\text{He}^*$, $(n, \alpha, n) {}^5\text{He}^*$ reactions and ${}^5\text{He}$ - ${}^5\text{He}$ double two body breakup process are shown in Fig. 2. The partial spectra after the eleventh level are not given in the Fig. 1 and Fig. 2 because of the small

values. The shape and energy of neutron spectra from different reaction mechanisms differ significantly from each other. The peak near 15 MeV mainly comes from the elastic scattering. The peak near 13 MeV mainly comes from the first, second, and fourth excited levels, while a wide spectrum is given by the third excited level with small values. The low energy region of total spectra are mainly come from the contribution of the second neutron emitted from $(n, 2n) {}^8\text{Be}^*$ (as shown in Fig. 1) and the ${}^5\text{He}$ breakup process (as shown in Fig. 2). Meanwhile, the direct three body breakup of ${}^6\text{He}$ also contributes to the low-energy region, but the direct three body breakup of ${}^{10}\text{Be}$ has a very wide spectrum from $0 \sim 14$ MeV, as shown in Fig. 1.

Although the updated level schemes [16] have been employed in this calculation, it should be noted that there are still some deficiencies. From Fig. 1 and Fig. 2, one can see that the calculated results are obviously lower than the experimental data of Ref. [7] in the energy region $4 \sim 7$ MeV, in which there are no contribution from any reaction mechanisms besides the direct three body breakup of ${}^{10}\text{Be}$ with wide spectrum through

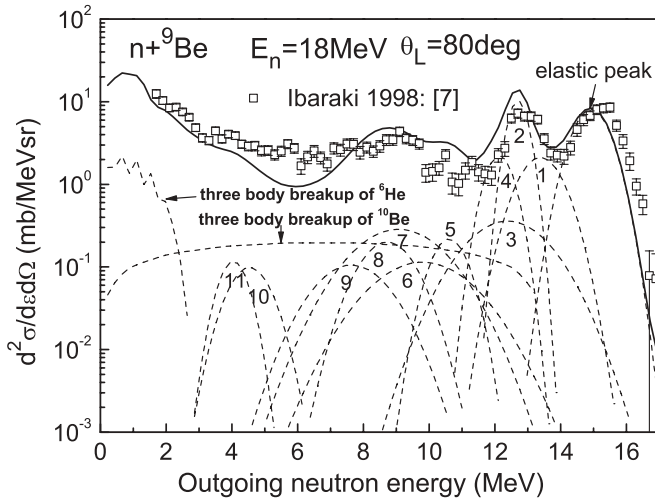


FIG. 1. The partial energy-angular spectra from $(n, 2n) {}^8\text{Be}^*$ reaction with outgoing angle of 80° at $E_n = 18$ MeV. The solid line corresponds to the calculated total outgoing neutron energy-angular spectrum, and square points correspond to the experimental data taken from Ref. [7]. The dash lines correspond to the partial neutron spectra of the first neutron emitted from $(n, 2n) {}^8\text{Be}^*$ and the direct three body breakup processes of ${}^6\text{He}^*$ and ${}^{10}\text{Be}^*$. The labels of 1 ~ 11 signify respectively the contributions of the excited level order numbers of the residual nucleus ${}^9\text{Be}^*$.

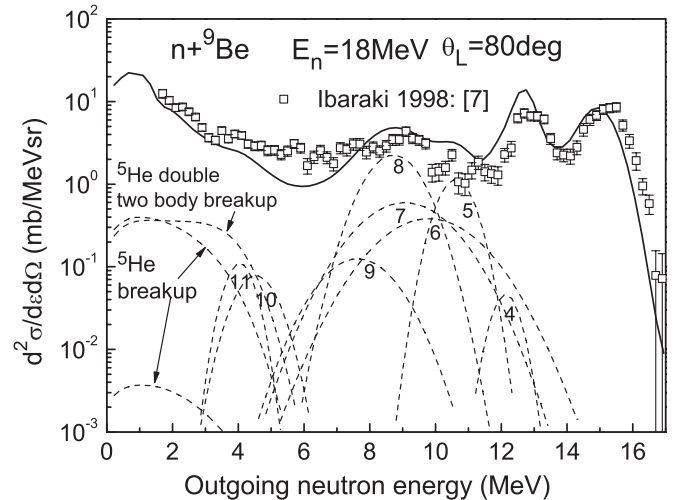


FIG. 2. The same as Fig. 1, but the partial energy-angular spectra from $(n, n\alpha) {}^5\text{He}^*$ reaction. The dash lines correspond to the partial spectra of the neutron emitted from the $(n, n\alpha) {}^5\text{He}^*$, ${}^5\text{He}$ breakup, and ${}^5\text{He}$ double two-body breakup reactions. The labels of 4 ~ 11 signify respectively the contributions of the excited level order numbers of the residue nucleus ${}^9\text{Be}^*$. The experimental data are taken from Ref. [7].

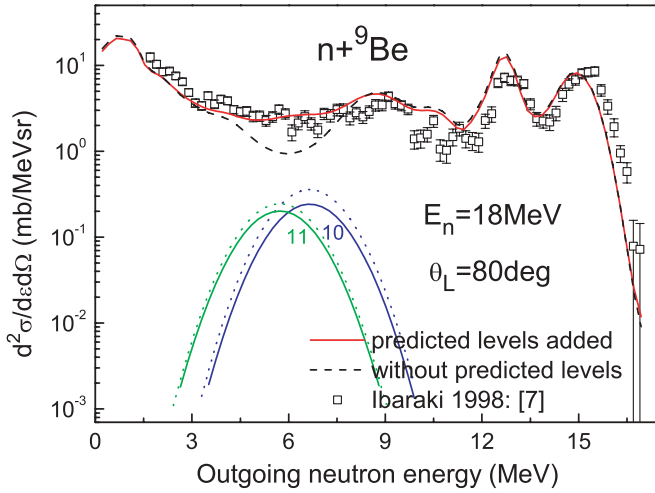


FIG. 3. (Color online) The comparison between the calculated results, which the predicted levels have been employed (red solid line) or not been employed (black dash line), and the experimental data taken from Ref. [7] with outgoing angle of 80° at $E_n = 18$ MeV. The blue solid and dot lines (denoting 10) correspond to the first neutron contribution from the predicted level $9.0({}_{2}^{5+})$ through $(n, 2n){}^8\text{Be}^*$ and $(n, n\alpha){}^5\text{He}^*$ reactions, respectively. The green lines do so but for the predicted level $10.0({}_{2}^{5+})$.

above analysis. On the other hand, the energy interval between the 9th and 10th excited level of ${}^9\text{Be}$ is up to 3.343 MeV as mentioned in Sec. I, which is much higher than the average energy interval. Therefore, in order to well reproduce the measurement data [5,7] at $E_n = 14.1$ and 18 MeV, two predicted levels of ${}^9\text{Be}$ about 9 and 10 MeV should be added. The comparisons between the calculated results that the predicted levels have been added or not are shown in Fig. 3 and Fig. 4 for incident neutron energy $E_n = 18$ and 14.1 MeV, respectively. The partial spectra from two predicted levels $9.0({}_{2}^{5+})$ and $10.0({}_{2}^{5+})$ have been denoted by 10 and 11 in Fig. 3 and Fig. 4. Obviously, the predicted levels $9.0({}_{2}^{5+})$

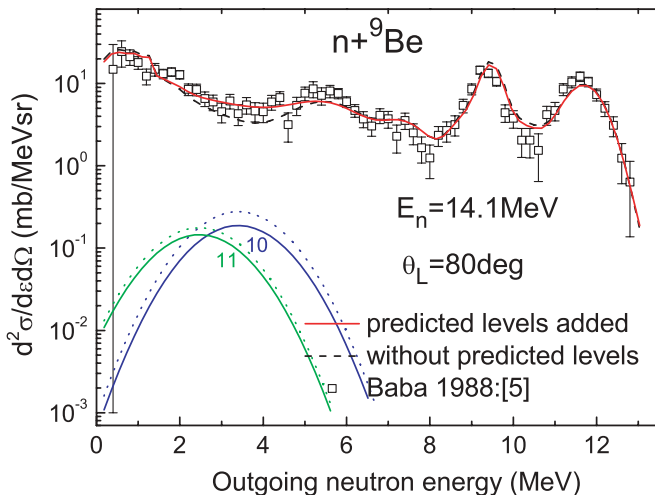


FIG. 4. (Color online) The same as Fig. 3 but at $E_n = 14.1$ MeV. The experimental data are taken from Ref. [5].

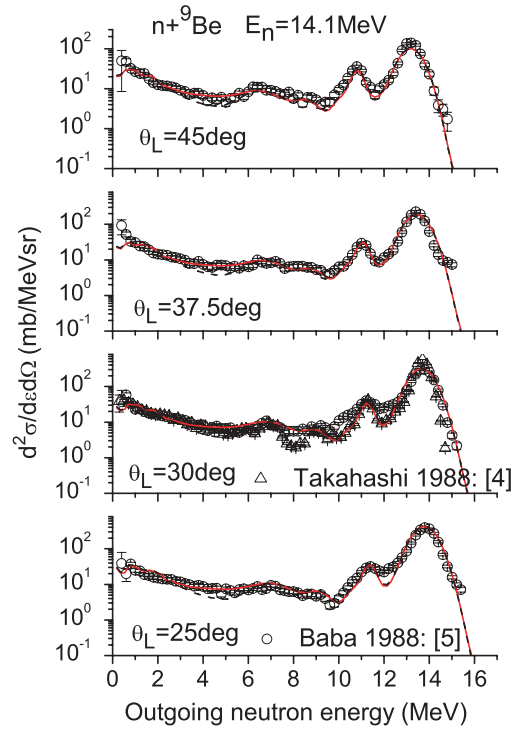


FIG. 5. (Color online) The energy-angular spectra of 25° , 30° , 37.5° , and 45° at $E_n = 14.1$ MeV. The red solid lines and the black dash line correspond to the results that the predicted levels have or not been added, respectively. The experimental data are taken from Ref. [4] (triangle) and from Ref. [5] (circle), respectively.

and $10.0({}_{2}^{5+})$ can emit the secondary neutron and α particle from $(n, 2n){}^8\text{Be}^*$ and $(n, n\alpha){}^5\text{He}^*$ reactions, respectively, so each level could give two neutron spectra. Therefore, four new outgoing neutron partial spectra are added. From Fig. 3 and Fig. 4, one can see that there are obvious contributions coming from the predicted levels to the total spectrum. And if they were absent in the model calculation, the results of total double-differential cross sections would deviate obviously from the experimental measurements in the outgoing neutron energy region $4 \sim 7$ MeV at $E_n = 18$ MeV and in the energy region $2 \sim 5$ MeV at $E_n = 14.1$ MeV. Moreover, the spins and parities of the predicted levels that are sensitive to calculation as shown in Eq. (2) are consulted by the spins and parities of adjacent levels and determined finally by fitting results.

The comparisons of the calculated results, which the predicted levels have been employed (red solid line) or not been employed (black dash line), with the experimental data measured by M. Baba [5] in 1988 are shown in Fig. 5 to Fig. 7 at $E_n = 14.1$ MeV for outgoing angles of 25° , 30° , 37.5° , 45° , 52.5° , 60° , 80° , 100° , 120° , 135° , and 150° , respectively. Meanwhile, the another set of experimental data measured by A. Takahashi in [4] at $E_n = 14.1$ MeV are also shown in above figures with the same outgoing angles of 30° , 60° , 80° , 100° , and 150° . The comparisons of the calculated results as mentioned above with the experimental data measured by M. Ibaraki [7] in 1998 are shown in Figs. 8 to 10 at $E_n = 18$ MeV for outgoing angles of 20° , 30° , 37.5° , 45° , 52.5° , 60° , 70° , 80° , 90° , 105° , 120° , 135° , and 150° ,

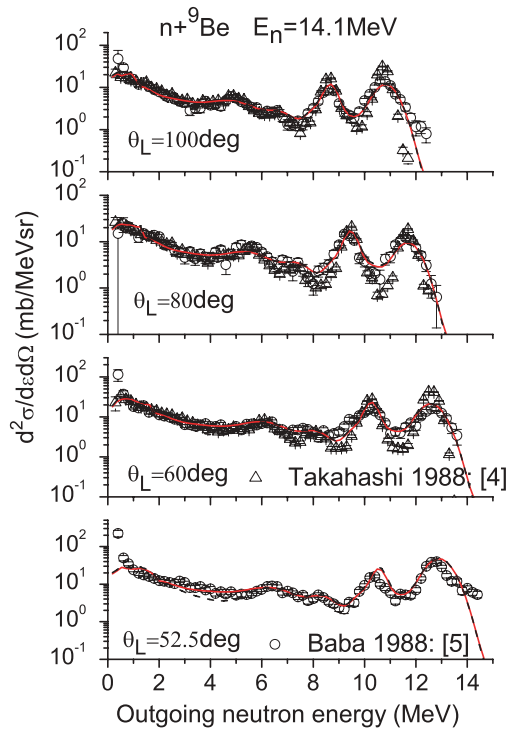


FIG. 6. (Color online) The same as Fig. 5 but for outgoing angles of 52.5°, 60°, 80°, and 100° at $E_n = 14.1$ MeV. The experimental data are taken from Ref. [4] (triangle) and from Ref. [5] (circle), respectively.

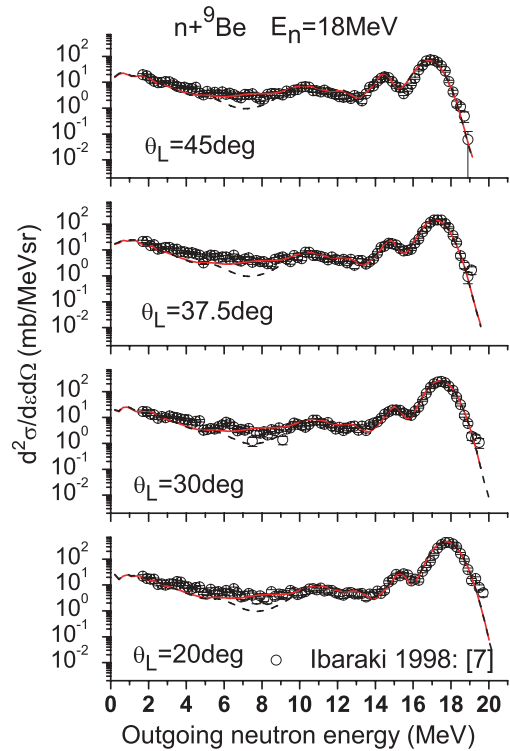


FIG. 8. (Color online) The same as Fig. 5 but for outgoing angles of 20°, 30°, 37.5°, and 45° at $E_n = 18$ MeV. The experimental data are taken from Ref. [7].

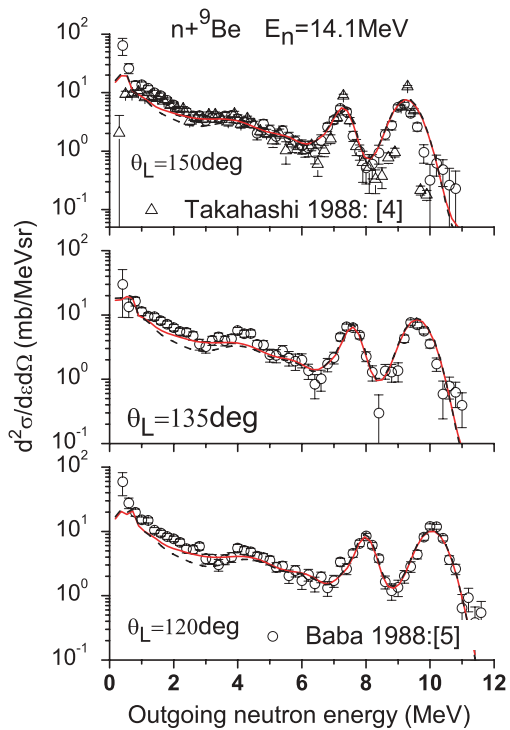


FIG. 7. (Color online) The same as Fig. 5 but for outgoing angles of 120°, 135°, and 150° at $E_n = 14.1$ MeV. The experimental data are taken from Ref. [4] (triangle) and from Ref. [5] (circle), respectively.

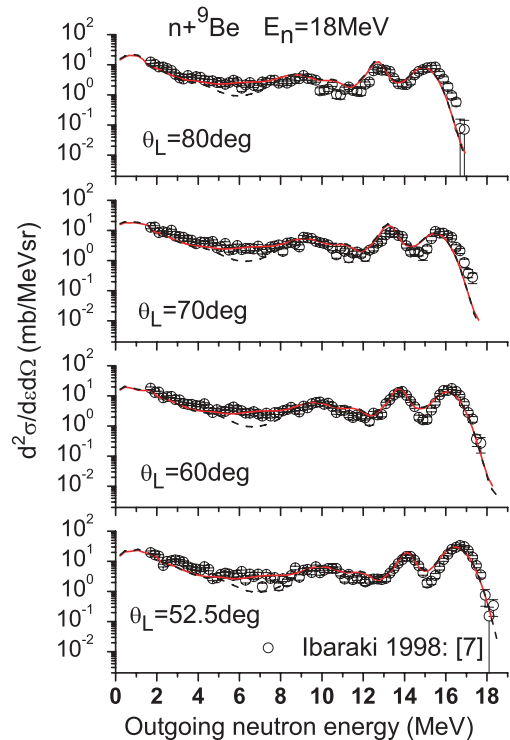


FIG. 9. (Color online) The same as Fig. 5 but for outgoing angles of 52.5°, 60°, 70°, and 80° at $E_n = 18$ MeV. The experimental data are taken from Ref. [7].

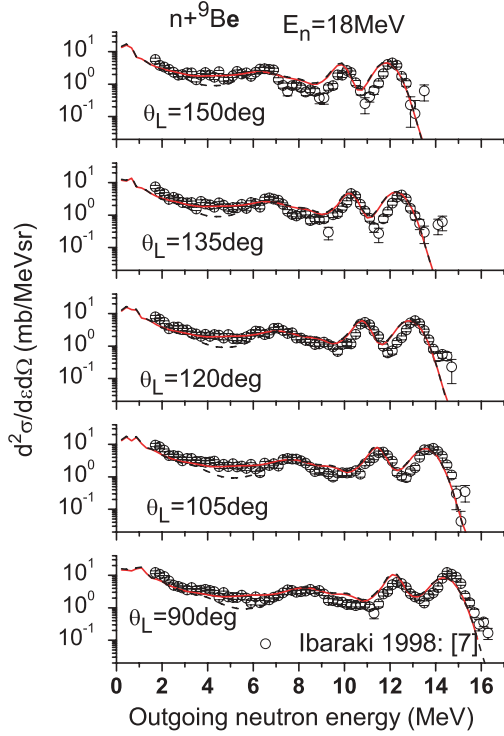


FIG. 10. (Color online) The same as Fig. 5 but for outgoing angles of 90° , 105° , 120° , 135° , and 150° at $E_n = 18$ MeV. The experimental data are taken from Ref. [7].

respectively. As shown in those figures all of the fittings agree very well with the measurements after the predicted levels $9.0(\frac{5}{2}^+)$ and $10.0(\frac{5}{2}^+)$ have been added to the level scheme of ${}^9\text{Be}$, otherwise the calculated results would deviate obviously from the experimental measurements.

V. SUMMARY

The total outgoing neutron energy-angular spectra for $n + {}^9\text{Be}$ reactions have been calculated and analyzed by the statistical theory for neutron induced-light nucleus reactions. In $n + {}^9\text{Be}$ reactions, the total outgoing neutron energy-angular spectra mainly come from the $(n, 2n)2\alpha$ reaction channel with six different reaction processes.

In light nucleus reactions, all of the residual states are discrete levels, therefore, the model calculations are very sensitive to the level schemes. Although the updated level scheme of ${}^9\text{Be}$ have been employed in the calculation, there are still some deficiencies between contributions from the 9th and 10th levels. In view of the much higher energy interval, we predict there are two new levels between the 9th level $7.94(\frac{5}{2}^-)$ and the 10th level $11.238(\frac{7}{2}^+)$. The calculated results indicate the fittings would be improved obviously while the predicted levels $9.0(\frac{5}{2}^+)$ and $10.0(\frac{5}{2}^+)$ have been employed in calculation. The spins, parities and energy widths of two predicted levels have been consulted by the values of adjacent levels and determined finally by fitting results, but they are not enough precise. At last, we hope these two predicted levels could be validated by experiment.

ACKNOWLEDGMENTS

This work was supported by the National Natural Science Foundation of China under Grant Nos. 10547005.

APPENDIX

There are only the particle waves with $l = \text{even}$ in an identical particle system. Since ${}^5\text{He}$ is unstable and breakup spontaneously into a neutron and an α particle with $Q_5 = 0.894$ MeV. We denote that m_n and m_α are the masses of neutron and α particles, respectively. M_5 is the mass of ${}^5\text{He}$. The calculation indicates that the dominant contribution of two ${}^5\text{He}$ is in their ground states. In this case the normalized double-differential cross sections of the neutron in center-of-mass system (CMS) has the form as

$$\frac{d^2\sigma}{d\varepsilon_n^c d\Omega_n^c} = \sum_{l=\text{even}} \frac{2l+1}{4\pi} f_l^c(\varepsilon_n^c) P_l(\cos\theta^c), \quad (\text{A1})$$

where P_l refers to the Legendre polynomial. The Legendre coefficients $f_l^c(\varepsilon_n^c)$ have been given by [17]

$$f_l^c(\varepsilon_n^c) = \frac{1}{4\gamma_n \varepsilon_n^r} f_l^{5\text{He}}(c) P_l(\eta_n), \quad (\text{A2})$$

where the Legendre coefficients $f_l^{5\text{He}}(c)$ of ${}^5\text{He}$ in CMS is calculated by using the unified Hauser-Feshbach and exciton model [17], and

$$\gamma_n = \sqrt{\frac{E_5^c m_n}{\varepsilon_n^r M_5}} \quad (\text{A3})$$

and

$$\eta_n = \sqrt{\frac{\varepsilon_n^r \varepsilon_n^c - 1 + \gamma_n^2}{\varepsilon_n^c 2\gamma_n}}. \quad (\text{A4})$$

In residual nucleus system (RNS) the neutron energy is Ref. [17]

$$\varepsilon_n^r = \frac{m_\alpha}{M_5} Q_5. \quad (\text{A5})$$

The energy of ${}^5\text{He}$ in CMS is given by

$$E_5^c = \frac{M_5}{M_{10}} (E^* - B_5), \quad (\text{A6})$$

where M_{10} is the mass of ${}^{10}\text{Be}$, and B_5 is the binding energy of ${}^5\text{He}$ in ${}^{10}\text{Be}$. E^* stands for the excitation energy of the compound nucleus

$$E^* = \frac{M_9}{M_{10}} E_n + B_n, \quad (\text{A7})$$

where M_9 is the mass of ${}^9\text{Be}$, and B_n is the binding energy of neutron in ${}^{10}\text{Be}$.

The minimum and the maximum energies of neutron in CMS are given by

$$\varepsilon_{n,\text{min}}^c = \varepsilon_n^r (1 - \gamma_n)^2; \quad \varepsilon_{n,\text{max}}^c = \varepsilon_n^r (1 + \gamma_n)^2. \quad (\text{A8})$$

For the α particles from two ${}^5\text{He}$ breakup process, the formula can be obtained by exchanging m_n and m_α . The velocity of the center of mass is $V_C = \frac{\sqrt{2m_n E_n}}{M_{10}}$.

In statistical physics the observable physical quantity is given by the averaged one over the distribution function. Therefore, the energy carried by each neutron in laboratory system (LS) is obtained by

$$\begin{aligned} E_n^l &= \int_{\varepsilon_n^c, \min}^{\varepsilon_n^c, \max} \frac{d^2\sigma}{d\varepsilon_n^c d\Omega_n^c} \frac{1}{2} m_n (\vec{v}_n + \vec{V}_C)^2 d\varepsilon_n^c d\Omega_n^c \\ &= \int_{\varepsilon_n^c, \min}^{\varepsilon_n^c, \max} f_0^c(\varepsilon_n^c) \left(\varepsilon_n^c + \frac{m_n m_n E_n}{M_{10}^2} \right) d\varepsilon_n^c \\ &= \frac{m_n m_n}{M_{10}^2} E_n + \frac{m_\alpha}{M_5} Q_5 + \frac{m_n}{M_5} E_5^c, \end{aligned} \quad (\text{A9})$$

and the energy carried by each α particle in LS is obtained by

$$E_\alpha^l = \frac{m_n m_\alpha}{M_{10}^2} E_n + \frac{m_n}{M_5} Q_5 + \frac{m_\alpha}{M_5} E_5^c. \quad (\text{A10})$$

Thus, the total released energy in LS is given by

$$E_{\text{total}}^l = 2E_n^l + 2E_\alpha^l = E_n + B_n - B_5 + 2Q_5. \quad (\text{A11})$$

The Q value of the $^{10}\text{Be} \rightarrow ^5\text{He} + ^5\text{He} \rightarrow 2n + 2\alpha$ reaction channel is

$$Q = B_n - B_5 + 2Q_5. \quad (\text{A12})$$

So the energy balance $E_{\text{total}}^l = E_n + Q$ is held strictly.

-
- [1] D. M. Drake *et al.*, Nucl. Sci. Eng. **63**, 401 (1977).
 [2] M. Baba *et al.*, in *Proceedings of the International Conference on Nuclear Physics/Reactor Data* (United Kingdom Atomic Energy Authority, Hawell, 1978), p. 198.
 [3] A. Takahashi *et al.*, Osaka University Report No. OKTAVIAN A-83-01, 1983; also see J. Nucl. Sci. Technol. **21**, 577 (1984).
 [4] A. Takahashi, Y. Sasaki, and H. Sugimoto, in *Proceedings of the 1987 Seminar on Nuclear Data, Tokai, 1988*, edited by T. Nakagawa and A. Zukeran (Japan Atomic Energy Research Institute, Tokai, 1988), p. 279.
 [5] M. Baba *et al.*, in *Proceedings of the International Conference on Nuclear Data for Science and Technology* (Mito, Japan, 1988), p. 209.
 [6] B. J. Qi *et al.*, At. Energy Sci. Technol. **29**, 315 (1995).
 [7] M. Ibaraki, M. Baba *et al.*, J. Nucl. Sci. Technol. **35**, 843 (1998).
 [8] X. C. Ruan *et al.*, High Energy Phys. Nucl. Phys. **31**, 442 (2007).
 [9] D. Schmidt, W. Mannhart, and S. Khurana, Physikalisch-Technische Bundesanstalt Report No. PTB-N-55, 2007.
 [10] J. X. Chen, P. Zhu *et al.*, Ann. Nucl. Energy **36**, 668 (2009).
 [11] S. T. Perkins, E. F. Plechaty, and R. J. Howerton, Nucl. Sci. Eng. **90**, 83 (1985).
 [12] T. D. Beynon and B. S. Sim, Ann. Nucl. Energy **15**, 27 (1988).
 [13] W. L. Sun and B. A. Zhang, At. Energy Sci. Technol. **29**, 360 (1995).
 [14] V. G. Pronyaev, S. Tagesen, and H. Vonach, in *Proceedings of the International Conference on Nuclear Data for Science and Technology, Bologna, 1997*, edited by G. Reffo, A. Ventura, and C. Grandi (SIF, Bologna, 1997), p. 268.
 [15] D. R. Tilley *et al.*, Nucl. Phys. **A708**, 3 (2002).
 [16] D. R. Tilley *et al.*, Nucl. Phys. **A745**, 155 (2004).
 [17] J. S. Zhang, Y. L. Han, and L. G. Cao, Nucl. Sci. Eng. **133**, 218 (1999).
 [18] J. S. Zhang, *Statistical Theory for Neutron Induced Light Nucleus Reaction* (Science Press, Beijing, 2009).
 [19] R. B. Firestone and V. S. Shirley, *Table of Isotopes, 8th ed.* (John Wiley & Sons, New York 1996).
 [20] J. F. Duan *et al.*, Commun. Theor. Phys. (submitted, 2009).
 [21] J. S. Zhang and Y. L. Han, Commun. Theor. Phys. **36**, 437 (2001).
 [22] J. S. Zhang and Y. L. Han, Commun. Theor. Phys. **37**, 465 (2002).
 [23] J. S. Zhang, Commun. Theor. Phys. **39**, 433 (2003).
 [24] J. S. Zhang, Commun. Theor. Phys. **39**, 83 (2003).
 [25] Y. L. Yan *et al.*, Commun. Theor. Phys. **44**, 128 (2005).
 [26] J. F. Duan *et al.*, Commun. Theor. Phys. **44**, 701 (2005).
 [27] J. F. Duan *et al.*, Commun. Theor. Phys. **47**, 102 (2007).
 [28] X. J. Sun *et al.*, Commun. Theor. Phys. **48**, 534 (2007).
 [29] X. J. Sun, W. Qu, J. Duan, and J. Zhang, Phys. Rev. C **78**, 054610 (2008).
 [30] J. S. Zhang and Y. Q. Wen, Chinese J. Nucl. Phys. **16**, 153 (1994).
 [31] J. S. Zhang *et al.*, Commun. Theor. Phys. **10**, 33 (1980).
 [32] J. S. Zhang, International Nuclear Data Committee Report, Report No. INDC(CRP) 014/LJ, 1990.
 [33] J. F. Duan *et al.*, Commun. Theor. Phys. **42**, 587 (2004).
 [34] G. G. Ohlsen, Instrum. Methods **37**, 240 (1965).